Presented at the 37th European PV Solar Energy Conference and Exhibition, 7-11 September 2020

SOLDERABLE PVD Al BACK CONTACTS FOR THE MODULE INTEGRATION OF HIGH-EFFICIENCY C-SI SOLAR CELLS

H. Nagel[1], S. Gledhill[1], T. Kroyer[1], Dirk Eberlein[1], A. Kraft[1],
T. Fischer[2], A. Hain[3], P. Wohlfart[3], M. Glatthaar[1] and S. W. Glunz[1]

[1] Fraunhofer Institute for Solar Energy Systems ISE, Heidenhofstr. 2, 79110 Freiburg, Germany
[2] teamtechnik Automation GmbH, Heinrich-Hertz-Straße 1, 71642 Ludwigsburg, Germany
[3] SINGULUS TECHNOLOGIES AG, Hanauer Landstrasse 103, 63796 Kahl am Main, Germany

ABSTRACT: Several high-efficiency solar cell types, such as tunnel oxide passivated contact and SunPower's interdigitaded back contact cells, benefit from physical vapour deposited (PVD) Al on the backside. For cell interconnection, the industry prefers to solder tinned Cu connectors to the cells' metal electrodes, so there is a great need to make the Al solderable. Cost calculations in a previous study have shown that the deposition of only one thin additional metal layer directly after the PVD of Al in the same coating system without interruption of the vacuum is the most cost-effective approach. In this work we introduce sputtered pure Ni as a solderable layer on PVD Al for the connection of c-Si solar cells. Using high-throughput tabber stringers we obtained a very high average normalised 90° interconnector peel force of 3.9 N/mm on our *p*-type PERC test cells. We also found a very good stability of the manufactured modules in climate tests carried out according to the standard IEC 61215. After double thermal cycling and damp-heat tests, the degradation of the electrical power was < 3 % for an only 100 nm thick pure Ni solderable layer.

Keywords: Physical Vapor Deposited Aluminum, Silicon Solar Cell, Module Integration

1 INTRODUCTION

Screen-printed and sintered back contacts are currently the most common for industrially manufactured crystalline silicon solar cells. They consist of large-area Al and local Ag solderable pads or an Ag grid. However, screen-printed and fired contacts have shortcomings, such as a possible reduction in the surface passivation of the cells due to the high sintering temperature and the penetration of metal into the otherwise well passivated silicon surfaces. This is especially true for tunnel oxide passivated contacts (TOPCon, a stack of tunnel oxide / polycrystalline Si / metal), which are today among the leading contact passivation technologies [1,2,3,4]. Physical vapor deposition (PVD) of Al is well suited for TOPCon, as metal spiking can be avoided. In addition, PVD-Al offers excellent back reflection of the infrared light passing through the cells. It is characterised by a very high electrical conductivity and on *n*- and *p*-type polycrystalline Si a low contact resistance can be achieved. As a result, a record power conversion efficiency of 26.1% was obtained for an interdigital back-contact (IBC) solar cell with PVD Al [5]. Other high-efficiency cell types also benefit from PVD Al back contacts including SunPower's IBC [6], the 'PassDop' cells introduced by Fraunhofer ISE, which achieve efficiencies of up to 23.5 % [7], and heterojunction solar cells [8].

For a broad industrial application of PVD Al a reliable and cost-effective interconnection technology is required. However, the soldering process preferred in industry is not easily possible with PVD Al because of the rapid formation of a native Al_2O_3 on its surface. The deposition of solderable metal on the Al is a common solution. Several materials and processes have already been investigated. In [9] a stack of PVD Al / ≥ 200 nm Ni : 7 wt% V / 20 nm Ag showed high peel forces of tinned Cu interconnectors that were soldered on. More than 4.5 N/mm were measured after 720 h of thermal treatment at 150 °C. In [10] peeling forces of more than 2 N/mm were achieved for a stack of PVD Al / ≥ 150 nm Ni:Si / 25 nm Ag. Passivated emitter and rear cells (PERC) with solderable sputtered 100 nm TiN / 20 nm Ti / 150 nm Ag or 100 nm TiN / 150 nm NiV / 15 nm Ag stacks on thermally evaporated Al back contacts were investigated in [11]. 200 thermal cycles and 1000 h damp-heat tests according to the IEC 61215 standard were passed by the modules prepared with the cells. In [12] a low specific contact resistance was achieved with PVD Al / 100 nm Ti / 400 nm Ag after 200 thermal cycles and 1000 h damp heat test.

Alternative deposition methods to PVD of the solderable metal on Al were also investigated. In [13] the PVD Al back contact of PERC cells was ultrasonically tinned. It was found that power degradation of cell strings laminated in standard glass-foil-modules was less than 5 % after double thermal cycling, damp heat and humidity freeze tests according to IEC 61215. Another approach is electroless metal deposition by a chemical displacement reaction [14,15]. In a simple and inexpensive dip-rinse-dry processing sequence, PVD Al was made solderable, achieving 90° peel forces > 2 N/mm.

With regard to process costs, it is advantageous if investments for production plants can be minimized. Cost calculations have shown that the deposition of only one thin additional metal layer on the PVD Al in the same coating system without interruption of the vacuum is the most cost-effective approach [16]. Therefore we investigated the performance of sputtered pure Ni as a single solderable layer on PVD Al for the interconnection of c-Si solar cells. High throughput tabber stringers were used for this purpose. We also tested NiV, which is easier to sputter than Ni, but not as solderable.

2 EXPERIMENTAL

We used ~20 % efficient front junction, alkaline textured *p*-type PERC CZ Si solar cells with screen-printed and sintered Ag front contacts and locally laser-fired PVD Al back contacts (LFC) on top of an electrically passivating 10 nm Al_2O_3 / 110 nm SiN stack. The approximately 1 µm thick Al rear contact was deposited in a high-rate inline vacuum system by thermal

evaporation. Due to availability of sputtering targets, we used another inline vacuum system for sputtering pure Ni onto the Al. The breaking of the vacuum after Al deposition creates a thin native Al_2O_3 film in between the Al and Ni layers. We assume that depositing Ni in the same coating system as Al without breaking the vacuum could result in an even more stable metal stack.

In an automated tabber-stringer TT4200 from teamtechnik, 1 mm wide Cu ribbons with SnPb coating were soldered onto the cells by means of controlled infrared lamp heating and connected to 3-cell-strings at a throughput of 2100 cells per hour per production track. Standard flux Kester 952s was used. The strings were laminated into photovoltaic modules with the cross-sectional construction soda-lime glass / ethylene vinyl acetate (EVA) / solar cells / EVA / PET-Al-PET backsheet. The illuminated *IV* curves of the modules were measured at standard test conditions (AM1.5, 1000 W/m², 25 °C) and electroluminescence (EL) images were taken under constant forward current. Measurements were carried out after light-induced degradation for 3 h under 1000 W/m² halogen lamp illumination at 85 °C and after subsequent damp heat and thermal cycling tests according to the IEC 61215 standard. The backsheet of a module was partially removed after thermal cycling test and the exposed back contacts of the cells were inspected by confocal optical microscopy. In addition, the resistances between the interconnectors and the back contacts were determined by four-point measurements with two coaxial Kelvin probes of 1 mm diameter spaced 5 mm apart.

The microstructure of a tinned Cu ribbon soldered on a PVD Al / pure Ni back contact of a PERC cell was studied by secondary electron microscopy (SEM) as well as energy dispersive X-ray spectroscopy (EDX). For this a cross section was prepared by ion milling.

On individual cells, which were not laminated into modules, the 90° interconnector peel force was measured and compared to the peel force measured on cells coated by a sputtered Ni : 7 wt% V layer instead of pure Ni. NiV was deposited in the same tool as the Al without breaking the vacuum. Tinned Cu ribbons were soldered manually onto NiV in contrast to the solar cells with pure Ni coating. It has to be noted that V or other elements are usually added to Ni sputter targets to make them non-magnetic and better suitable for magnetron sputtering. With magnetic targets part of the magnetic flux is shunted and thus reduced in front of the target. To overcome this problem we used a 1.5 mm thin pure Ni target. There are other technical solutions available, e. g. targets with multiple gaps [17] or magnets that are located outside the sputter target [18].

3 RESULTS AND DISCUSSION

3.1 Interconnector peel force

Fig. 1 shows the measured 90° peel force vs. distance curves for tinned Cu ribbons manually soldered on the PVD Al back contact of the PERC CZ Si solar cells with 100 nm sputtered NiV solderable layer. If the outer cell edges are neglected the peel force normalised to the ribbon width is higher than 0.6 N/mm everywhere and averages 2.2 N/mm. The standard DIN EN 50461 is well met which requires at least 1 N/mm on average. In some areas the tinned Cu ribbon separated from the NiV indicating a locally poorer soldered joint, whereas in areas with higher peel force the solar cell was peeled off the adhesive on the glass plate, see Fig. 2.

In experiments performed with a high-throughput tabber stringer we obtained much lower peel forces and in some cases there was even no adherence of the tinned Cu ribbon on the NiV layer at all. We attribute this to the V content, since V is a non-precious metal and a passivating oxide is formed in air on pure V. In the high-throughput tabber-stringer the interaction time between NiV, SnPb and flux is short and so the oxide layer may not be removed.

In contrast, pure nickel is much more stable. It is highly resistant to air, at room temperature there is only a very thin oxide formed on its surface [19] that does not hinder soldering. We measured average normalised peel forces of 3.5 N/mm for 50 nm thick Ni (Fig. 3) and 3.9 N/mm for 100 nm thick Ni solderable layer (Fig. 4), i. e. at least 1.3 N/mm higher than for NiV. At each point, the interconnector together with the soldered solar cell was

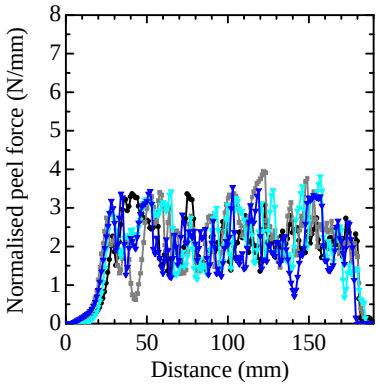

Fig. 1: Measured 90° peel force vs. distance for tinned Cu ribbons manually soldered on the PVD 1 µm Al / 100 nm NiV back contact of PERC CZ Si solar cells. Every curve represents the data obtained for one connector.

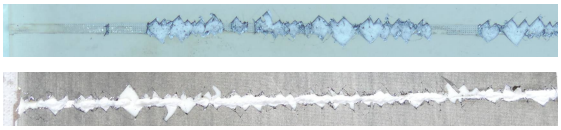

Fig. 2: Photographs of the backside of PERC with 100 nm NiV (top) or 100 nm pure Ni solderable layer (bottom) on the 1 µm thick PVD Al rear contact after the interconnector peel test.

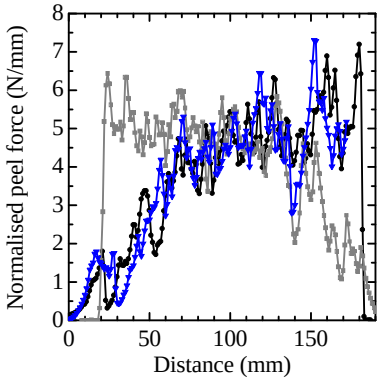

Fig. 3: Measured 90° peel force vs. distance for tinned Cu ribbons soldered on the PVD 1 µm Al / 50 nm Ni back contact of PERC using a high-throughput tabber stringer.

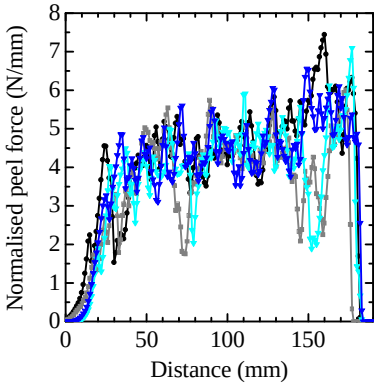

Fig. 4: Measured 90° peel force over distance for tinned Cu ribbons soldered on the PVD 1 µm Al / 100 nm Ni back contact of PERC CZ Si solar cells using a high-throughput tabber stringer.

removed from the glass plate to which the cell was glued (Fig. 2 bottom). Thus, the measured peel force was limited by the adhesive on the glass plate and the soldered joint of the interconnector on the cells was even stronger than the values shown in Figs. 3 and 4.

3.2 Module climate tests

Two types of 3-cell photovoltaic modules have been produced from solar cells with either 50 nm or 100 nm thick pure Ni solderable layer on the PVD Al. After light-induced degradation (LID) the modules were subjected to a damp heat test at 85 °C and 85 % relative humidity or a temperature cycling test between -40 °C and 85 °C. Fig. 5 top shows the electrical power at maximum power point (P_{mpp}), the open-circuit voltage (V_{oc}), the short-circuit current density (J_{sc}) and the fill factor (*FF*) of the prepared 3-cell-strings in the modules with 50 nm solderable layer measured under standard test conditions. After 2000 h in the damp heat test, which is twice the testing time specified in the IEC 61215 standard, no power degradation was observed. Obviously a possible ingress of moisture into the module together with elevated temperature did not damage the soldered joints. The EL images show excellent stability against the applied stress everywhere in the cells (Fig. 5 bottom).

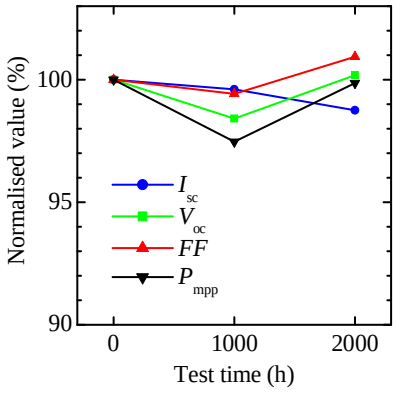

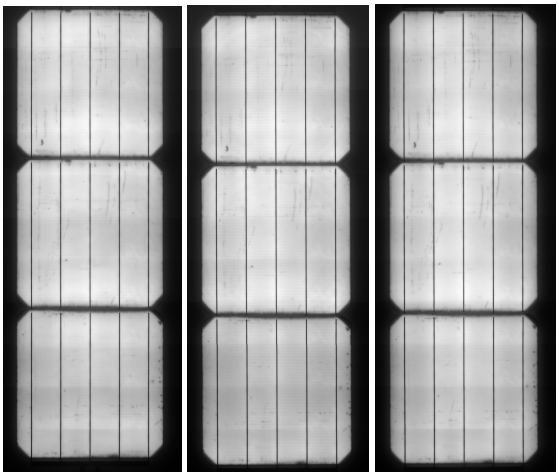

Fig. 5: Measured illuminated *IV* parameters (top) and EL images (bottom), taken under forward current, of the same 3-cell-module before (left), after 1000 h (middle) and after 2000 h (right) in the damp heat test. The thickness of the Ni layer was 50 nm.

The results of the thermal cycling test are different. After 200 cycles, as required by the standard, the *FF* and P_{mpp} degradation are already 3.3 % and 1.7 % relative, respectively (Fig. 6 top). After 400 cycles, the power degradation due to *FF* loss increased to 8 %. The reason is an increase in series resistance. The EL images show strip-shaped dark areas between some outer interconnectors and cell edges (Fig. 6 bottom). The conductive connection between interconnectors and solar cell metallization is interrupted on this side of the interconnectors whereas on the other side of the interconnectors the conductive connection is intact since

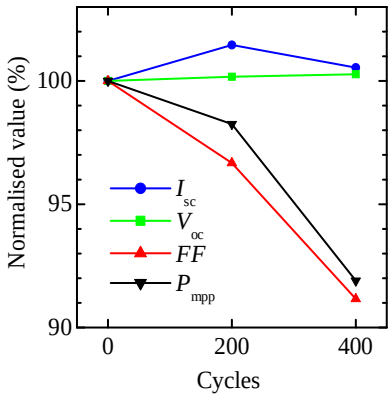

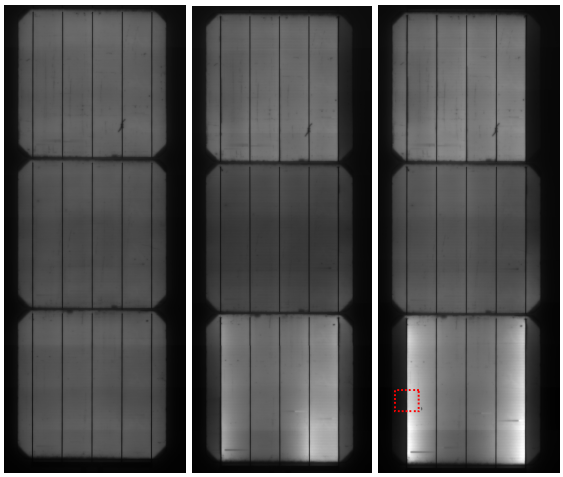

Fig. 6: Measured illuminated *IV* parameters (top) and EL images (bottom), taken under forward current, of the same 3-cell-module before thermal cycle test (left), after 200 (middle) and after 400 temperature cycles (right). The thickness of the Ni layer was 50 nm. The red square marks the position of the microscope images shown in Fig. 7.

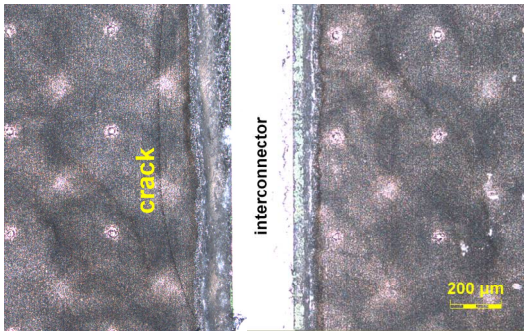

Fig. 7: Optical microscope images taken from the 1 µm Al / 50 nm Ni back contact after 400 thermal cycles and removal of the backsheet. Left: Low EL intensity on the front side. Right: High EL intensity on the front side. The bright spots are laser-fired contacts.

the EL intensity is high there. Obviously, the interconnectors were not detached from the cells' metallization but rather the cells' metallization was interrupted on one side of the interconnectors. This is confirmed by optical microscopy of the back contacts of the cells after removal of the backsheet. In all the places we investigated, we found cracks only on the side of the interconnectors where the EL intensity is low. Examples of microscope images are shown in Fig. 7. They were taken from the lower cell of the string depicted in Fig. 6. It should be noted that we cannot exclude the possibility

Table 1: Resistances measured on the rear of the module containing cells with 1 µm Al / 50 nm Ni back contact (BC) after 400 thermal cycles and removal of the backsheet. The distance between the coaxial *IV* probes was 5 mm.

***IV* probe 1 on**	***IV* probe 2 on**	**Resistance (Ω)**
Back interconnector	BC, high EL intensity on the front	0.02
Back interconnector	BC, low EL intensity on the front	0.25 to 0.55
BC, high EL intensity on the front	BC, low EL intensity on the front	0.27 to 0.75

that the cracks found may have been enlarged or even caused by the force exerted when peeling the backsheet.

The resistance measured between interconnector and back contact area with high EL intensity on the front side is low, whereas it is significantly higher when measuring between interconnector and back contact area with low EL intensity, see Table 1. The resistance of the back contact between areas with high and low front side EL intensity is also high. This behavior can be well explained by the observed cracks, which interrupt the back contact only on one side of the interconnector. Note that it can be assumed that the cracks extend to the front of the solar cell and that the front contact grid is interrupted as well. It is possible that locally alternating

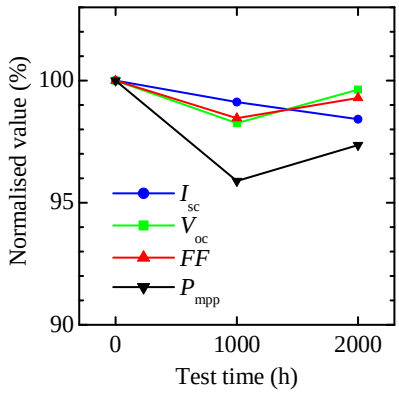

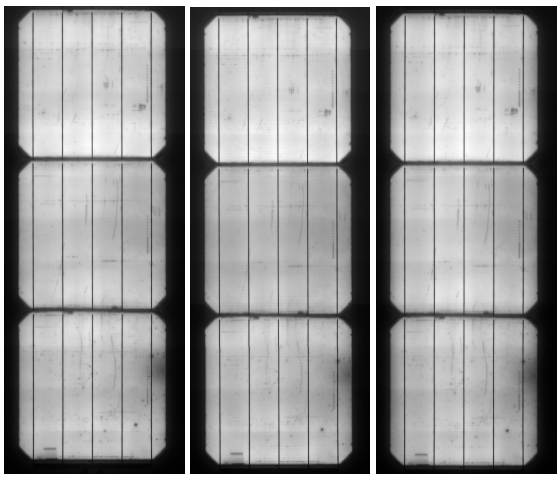

Fig. 8: Measured illuminated *IV* parameters (top) and EL images (bottom), taken under forward current, of the same 3-cell-module before (left), after 1000 h (middle) and after 2000 h (right) in the damp heat test. The thickness of the Ni layer was 100 nm.

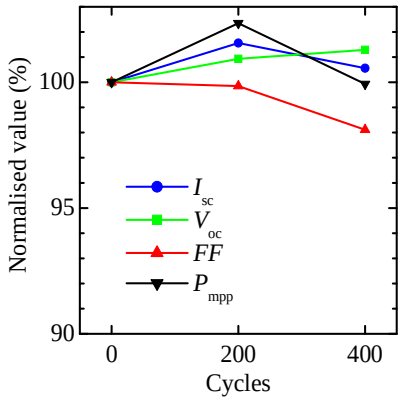

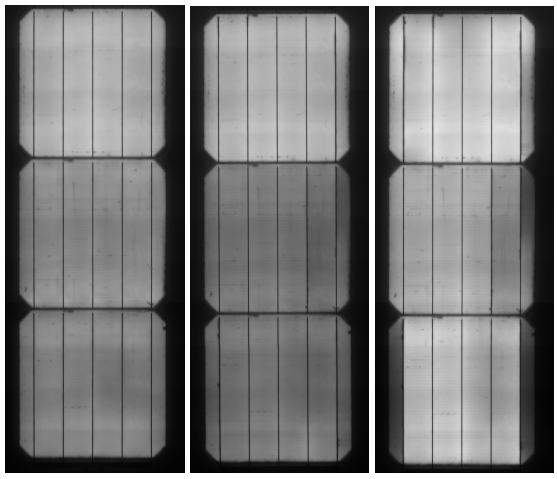

Fig. 9: Measured illuminated *IV* parameters (top) and EL images (bottom), taken under forward current, of the same 3-cell-module before thermal cycle test (left), after 200 (middle) and after 400 temperature cycles (right). The thickness of the Ni layer was 100 nm.

strong and weak bonds in the back contact are the cause for the formation of cracks, as discussed in Section 3.3.

Figs. 8 and 9 show the course of the electrical performance parameters for 100 nm pure Ni solderable layer. After double thermal cycling and damp-heat tests, the electrical power degradation was < 3 % in this case. As with 50 nm Ni, the EL images show perfect local stability in the damp heat test. After 400 thermal cycles, the *FF* decreased by 2 % relative. Since the power degradation is significantly below 5 %, the strings with 100 nm thick pure Ni layer can be considered very stable. The EL images of 2 cells disclose the beginning of interruption of the cell metallization as was observed in the previous test with 50 nm Ni. Here too, it should be noted that the asymmetrical EL images cannot be explained by large area separation of the interconnectors from the back contact.

3.3 Microstructure of the Al / Ni rear contact

The thinner the Ni layer, the higher the failure probability in the thermal cycling test. To find the reason for this, we examined the microstructure of the back contact using SEM. It is important to mention that after alkaline texture and an acid etching of the rear side for *pn*-isolation there are flattened random pyramids on the Si substrate with a roughness on a scale of 1 to 10 µm. The deposition of dielectric passivation layers on the backside does not change the microstructure of the surface since this layer stack is very thin (120 nm). However, the deposited Al features a multi-grain structure and its surface roughness has a structure size of about 200 nm (Fig. 10 top). We assume that the well known self-shading effect of Al evaporated on inclined planes is the reason for this. After deposition of 50 nm Ni the surface structure in the SEM looks similar (Fig. 10 bottom). However, the EDX image taken from a cross section after soldering tinned Cu ribbon upon the cell's back contact indicates that the structure of the Ni layer is very granular (Fig. 11 bottom). In analogy to the Al we assume that the reason for this is micro-shading by the rough surface during Ni deposition. Despite the granular Ni layer, close material connections of Ni and Al with the SnPb solder above were found. If one justifiably assumes a low adhesion of tin and a high adhesion of Ni to Al, very high local mechanical stresses are the result in the thermal cycling test that might crack the Si substrate as was found in Section 3.2. Note that the shear forces of the tinned Cu interconnector in the TCT are very high due to the 6 times higher thermal expansion coefficient compared to Si.

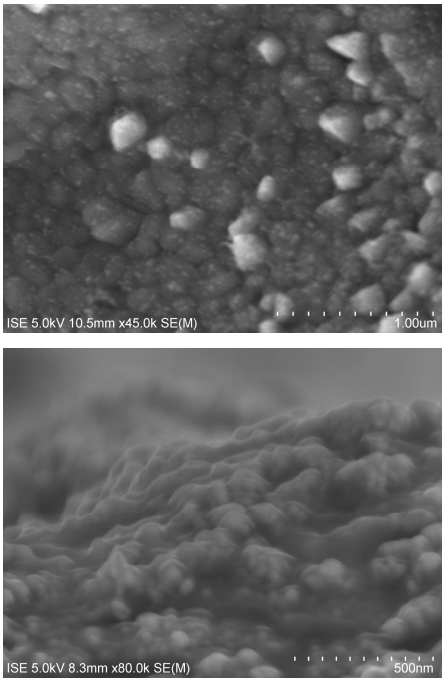

Fig. 10: SEM images of the backside of a PERC cell with 1 µm PVD Al back contact before (top) and after (bottom) sputter deposition of 50 nm Ni.

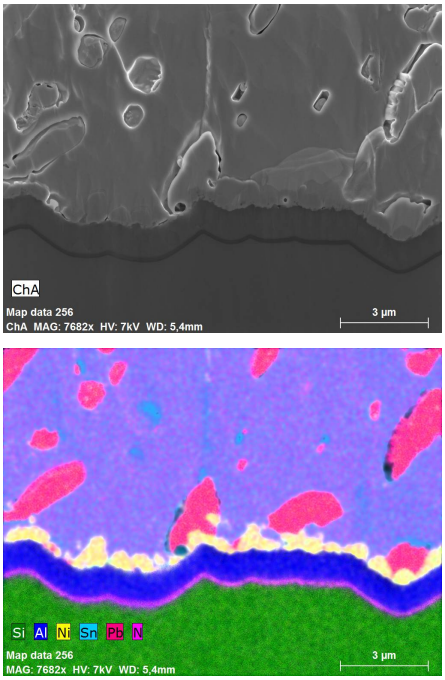

Fig. 11: SEM (top) and EDX images (bottom) of a cross-section of a copper ribbon with SnPb coating soldered to the rear side of a PERC c-Si solar cell with 10 nm Al_2O_3 / 110 nm SiN dielectric passivation stack, 1 µm thermally evaporated Al and 50 nm thick (on an average) sputtered Ni.

4 SUMMARY AND CONCLUSION

A thin PVD pure Ni layer is well suited for making the PVD Al back contact of c-Si solar cells solderable. The measured average normalised 90 ° peel force of tinned Cu interconnectors soldered onto the PVD 1 µm Al / 100 nm Ni rear contact of *p*-type PERC cells was 3.9 N/mm, which meets the standard DIN EN 50461 (> 1 N/mm). In addition, the stability of glass/foil-modules manufactured with such cell strings in climate tests was very high. After double thermal cycling and damp-heat tests the electrical power degradation was less than 3 %, exceeding the standard IEC 61215 (< 5 % after 100 % of the tests). The microstructural investigations show that very high stability could also be achieved with much thinner Ni layers if their thickness uniformity is improved.

Considering the good performance of PVD Al e. g. on TOPCon solar cells with the highest efficiency of 26.1 % [1] and the only slightly higher deposition costs

of Al / Ni compared to Al / NiV (which is about 5 €Cent/wafer as described in [2]) because the thin pure Ni sputter target has to be exchanged more often than the NiV target, the presented technology is a good candidate for future industrial backside metallization of high-efficiency c-Si solar cells.

ACKNOWLEDGEMENT

The authors thank all colleagues at Fraunhofer ISE who contributed to this work and the German Federal Ministry for Economic Affairs and Energy for funding within the project 'IdeAl' under contract number 0325889B.

5 REFERENCES

[1] F. Feldmann, M. Bivour, C. Reichel, M. Hermle and S. W. Glunz, Passivated rear contacts for high-efficiency *n*-type Si solar cells providing high interface passivation quality and excellent transport characteristics, *Solar Energy Materials and Solar Cells* **120**, 270 – 274 (2014).

[2] J. Schmidt, R. Peibst and R. Brendel, Surface passivation of crystalline silicon solar cells: Present and future, *Solar Energy Materials and Solar Cells* **187**, 39 – 54 (2018).

[3] H. E. Çiftpinar, M. K. Stodolny, Y. Wu, G. J. M. Janssen, J. Löffler, J. Schmitz, M. Lenes, J.-M. Luchies and L. J. Geerligs, Study of screen printed metallization for polysilicon based passivating contacts, *Energy Procedia* **124**, 851 – 861 (2017)

[4] H.-C. Chang, C.-C. Lo, B.-C. Kung, S.-T. Liao, C.-J. Huang, C.-L.Cheng and M.-T. Kuo, Poly-Si passivated solar cells fabricated by firing contact metallization with shallow silver penetration, *Proceedings of the 36th EU Photovoltaic Solar Energy Conference*, 575 – 579 (2019)

[5] F. Haase, C. Hollemann, S. Schäfer, A. Merkle, M. Rienäcker, J. Krügener, R. Brendel, R. Peibst, Laser contact openings for local poly-Si-metal contacts enabling 26.1%-efficient polo-IBC solar cells, *Solar Energy Materials and Solar Cells* **186**, 184 − 193 (2018).

[6] W. P. Mulligan, M. J. Cudzinovic, T. Pass, D. Smith and R. M. Swanson, Metal contact structure and method of manufacture, patent application WO 2004 095 587 A3.

[7] B. Steinhauser, M. Kamp, A. Brand, U. Jäger, J. Bartsch, J. Benick and M. Hermle, High-efficiency *n*-type silicon solar cells: advances in PassDop technology and NiCu plating on boron emitter, *IEEE J. of Photovoltaics* **6,** 419 – 425 (2016).

[8] J.-C. Stang, M.-S. Hendrichs, A. Merkle, R. Peibst, B. Stannowski, L. Korte and B. Rech, ITO-free metallization for interdigitated back contact silicon heterojunction solar cells, *Energy Procedia* **124,** 379 – 383 (2017).

[9] V. Jung and M. Köntges, Al/Ni:V/Ag metal stacks as rear-side metallization for crystalline silicon solar cells, *Progress in Photovoltaics* **21**, 876 – 883 (2013).

[10] V. Jung, F. Heinemeyer, M. Köntges and R. Brendel, Ni:Si as barrier material for a solderable PVD metallization of silicon solar cells, *Energy Procedia* **38**, 362 – 367 (2013).

[11] J. Kumm, R. V. Chacko, H. Samadi, P. Hartmann, D. Eberlein and A. Wolf, Long-term and annealing stable, solderable PVD metallization with optimized Al diffusion barrier, *Energy Procedia* **77**, 374 – 381 (2015).

[12] T. Geipel, J. Kumm, M. Moeller, L. Kroeley, A. Kraft, U. Eitner, A. Wolf, Z. Zhang and P. Wohlfart, Low-temperature interconnection of PVD aluminium metallization, *Energy Procedia* **98**, 125 – 135 (2016).

[13] H. Nagel, D. Eberlein, S. Hoffmann, M. Graf, B. Steinhauser, F. Feldmann, A. Kraft, U. Eitner, M. Glatthaar, M. Hermle, S. W. Glunz, H. Haverkamp, T. Fischer, A. Hain, P. Wohlfart, V. Mertens, J. M. Müller and T. Buck, Ultrasonically tinned PVD Al rear contacts on high-efficiency crystalline silicon solar cells for module integration, *Proceedings of the 33rd EU Photovoltaic Solar Energy Conference*, 295 – 299 (2017).

[14] H. Nagel, M. Kamp, D. Eberlein, A. Kraft, J. Bartsch, M. Glatthaar and S. W. Glunz, Enabling solderability of PVD Al rear contacts on high-efficiency crystalline silicon solar cells by wet chemical treatment, *Proceedings of the 32nd EU Photovoltaic Solar Energy Conference*, 48 – 52 (2017).

[15] H. Nagel, J. Bartsch, M. Kamp, and M. Glatthaar, Method for interconnecting solar cells, patent application WO 2017 220 444 A3.

[16] A. Hain, H. Nagel, M. Doerr, T. Buck, Z. Peng, R. Lorenz, T. Fischer, S. Gledhill, T. Kroyer, M. Huber and P. Wohlfart, PVD metallization for high-efficiency c-Si solar cells: scenario for implementation in production, *Proceedings of the 35th EU Photovoltaic Solar Energy Conference*, 810 – 813 (2018).

[17] K. Nakamura, T. Yamada, Y. Ohta and A. Itoh, "GT target", a new high-rate sputtering target of magnetic materials, *IEEE Transactions on Magnetics* **18**, 1080 – 1082 (1982).

[18] K. Kawabata, T. Tanaka, A. Kitabatake, K. Yamada, Y. Mikami, H. Kajioka and K. Toiyama, High rate sputtering for Ni films by an rf-dc coupled magnetron sputtering system with multipolar magnetic plasma confinement, *J. Vac. Sci. Technol. A* **19**, 1438 – 1441 (2001).

[19] E. S. Lambers, C. N. Dykstal, J. M. Seo, J. E. Rowe and P. H. Holloway, Room-temperature oxidation of Ni(111) at low and atmospheric oxygen pressures, *Oxidation of Metals* **45**, 301 – 321 (1996).